

The corner element in classical elasticity and Cosserat elasticity

R. S. Lakes

December 31, 2021

Abstract

The corner element is considered in torsion of a square cross section bar. Understanding the corner element has a pedagogic role in mechanics of materials and elasticity and is also helpful in providing physical insight for generalized continuum theories such as Cosserat elasticity. Analysis of the corner element reveals the slope of the warp curve at the corner in a classical solid and approximates the slope of the warp curve in a Cosserat solid.

Preprint, *Journal of Mechanics of Materials and Structures (JOMMS)*, 16 (2) 225-235 (2021).
<https://doi.org/10.2140/jomms.2021.16.225>

1 Introduction

Corner elements are of interest for pedagogic reasons in classical elasticity and in relation to concentration of stress and strain in Cosserat elasticity.

The corner of a classical elastic rectangular block subject to a uniformly distributed shear stress on one surface and zero stress on the orthogonal surface exhibits a singular gradient of stress [1]. The singularity arises because the assumed boundary conditions are incompatible with the classical symmetry of the stress. Gradients of stress on a corner element balance out the moment due to the asymmetric surface stress. No matter how small the corner element, the gradient provides balance, because it diverges near the corner. At the corner, there is a discontinuity in the stress and a logarithmic singularity in the rotation [2]. If couple stress is allowed, as it is in Cosserat elasticity, the stress can be asymmetric due to surface moments on the corner element. The singularity is thereby eliminated [2].

The interior corner in an angle bar comprised of two orthogonal thin plates exhibits a singular shear stress when the bar is subject to torsion [3]. As the radius of curvature of the reentrant corner decreases, the stress concentration factor increases without bound. An elastic circular cylinder bonded to a half space exhibits a singular stress [4, 5, 6] in the vicinity of the reentrant corner. Stress concentration has been analyzed for torsion of a linear elastic solid with a dilute concentration of voids parallel to the torsion axis [7]. Some of the voids have interior corners.

Exterior corners give rise to zero stress. In particular, the corners of a square or rectangular cross section bar in torsion undergo zero stress and strain in connection with warp. Warp of cross sections of bars of non-circular cross section occurs in torsion as is well known in elasticity theory. The displacement field for torsion of a bar is as follows, with u_z as the warp and θ as the twist angle per length.

$$u_x = -\theta zy, \quad u_y = \theta zx, \quad u_z = \theta f(x, y) \quad (1)$$

For a bar of square cross section, the exact solution [3] [8] is, with $k_n = \frac{(2n+1)\pi}{A}$ and A as the full width of the bar,

$$u_z = \theta \left(xy - \sum_{n=0}^{\infty} \frac{8(-1)^n}{A \left(\frac{(2n+1)\pi}{A} \right)^3} \frac{\sinh k_n y}{\cosh(k_n A/2)} \sin k_n x \right). \quad (2)$$

The warp at a lateral surface is given by setting $y = \frac{A}{2}$. The corresponding strain is zero at the corners and attains a maximum on the center lines of the lateral surfaces. The stress is also zero at the corners. The full solution is, however, not needed to demonstrate zero stress and strain at the corners.

It is known that in Cosserat solids, via approximate solutions [9] [10] for a square cross section bar, the warp in torsion is reduced compared with the classical prediction. The result is that the peak strain at the center line of the lateral surfaces is reduced, and strain (as well as stress) spills over into the corners of the cross section where it is classically forbidden. Concentrations of stress and strain in torsion of the Cosserat elastic bar are reduced in comparison with a classical elastic solid. Stress concentration around holes in a plate under tension or shear is also reduced [11] in Cosserat solids compared with classical elastic solids. It is known that materials such as bone and foam exhibit reduced concentrations of stress and strain. This could result in an increase in toughness. In foams, toughness increases with the size of cells [12] and the Cosserat characteristic length increases with the size of cells [13]. However a direct demonstration of a reduced rate of energy release in a Cosserat solid compared with a corresponding classical solid is not known.

The corner is therefore of interest in several distributions of stress and strain in generalized continuum mechanics as well as in a pedagogic context in classical elasticity. In the present research, warp of cross sections of a square bar at the corner are analyzed for torsion in classical elasticity and in Cosserat elasticity.

2 Classical elastic torsion

2.1 Corner element: qualitative

There must be warp of cross sections of a square section bar in torsion because if there were not, stress would appear at the corner. The corner differential element is shown in Figure 1. There can be no shear stress at the corner because the lateral surfaces $x = \pm a$, $y = \pm a$ are free surfaces with no applied shear forces. The half width of the bar is $a = \frac{A}{2}$. Because the bar is subject to torsion, there must be shear stress and strain away from the corner. Therefore warp of the cross section must occur. This qualitative argument is traditionally used for didactic purposes in mechanics of materials courses in which the rigor of the exact solution would be onerous.

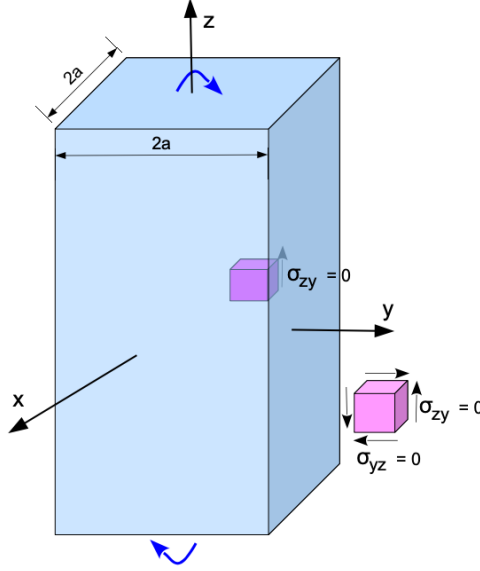


Figure 1: Stress vanishes at the corner of a cross section of a classically elastic square cross section bar in torsion.

2.2 Corner element: analysis

In the vicinity of the corner $(x, y) = (a, a)$, a linear warp function, equation 3, suffices to eliminate strain, hence stress at the corner.

$$u_z = -\theta a (-x + y) \quad (3)$$

This implies, with equation 1, zero shear strain $\epsilon_{yz} = \frac{1}{2}(\frac{\partial u_y}{\partial u_z} + \frac{\partial u_z}{\partial u_y})$. Because stress is proportional to strain, the linear warp satisfies the surface boundary condition for stress $\sigma_{yz}|_{y=a} = 0$. The slope of the line corresponds to the slope of the warp curve at the corner from the exact solution as shown in Figure 2. So, with little more effort than the qualitative argument for the existence of warp, once can obtain the slope of the warp curve at the corner. Thus far the displacement field represents a rotation, not torsion; it can only be representative of torsion at the corner.

With only a little more complexity, the warp function in equation 4 also achieves zero stress at the corner, and has an appropriate shape to represent warp.

$$u_z = \theta \frac{C_1}{2a^2} (x^3 y - x y^3) \quad (4)$$

This also obeys the equilibrium equations for elasticity

$$\sigma_{ij,i} = 0. \quad (5)$$

The shear stress on the surface $y = a$ is, with C_1 as a constant,

$$\sigma_{yz}|_{y=a} = G \frac{1}{2} \left(\theta x + \theta \frac{C_1}{2a^2} x^3 - \theta \frac{C_1}{2a^2} 3x a^2 \right). \quad (6)$$

The boundary condition $\sigma_{yz}|_{y=a} = 0$ for $x = \pm a$ is satisfied if $C_1 = 1$. Equation 4 has the correct slope at the corner as shown in Figure 2. The function has the appropriate sigmoid shape

for the warp but, because it was adjusted to satisfy the boundary conditions only at the corner, its peak value is too large compared with the classical curve and the slope at the center of the cross section does not match the classical value.

For points along the surface center line, $(x, y) = (0, a)$ the stress σ_{yz} , but not σ_{xz} , is identically zero. Consider a differential element nearby, $(x, y) = (\delta x, a)$. Enforcing the boundary condition $\sigma_{yz}|_{y=a} = 0$ gives $C_1 = \frac{2}{3}$; the slope of the warp curve then is correct in comparison with the exact solution near the center line but not at the corners. To obtain the correct slope at corners and surface center line one could incorporate a higher order term.

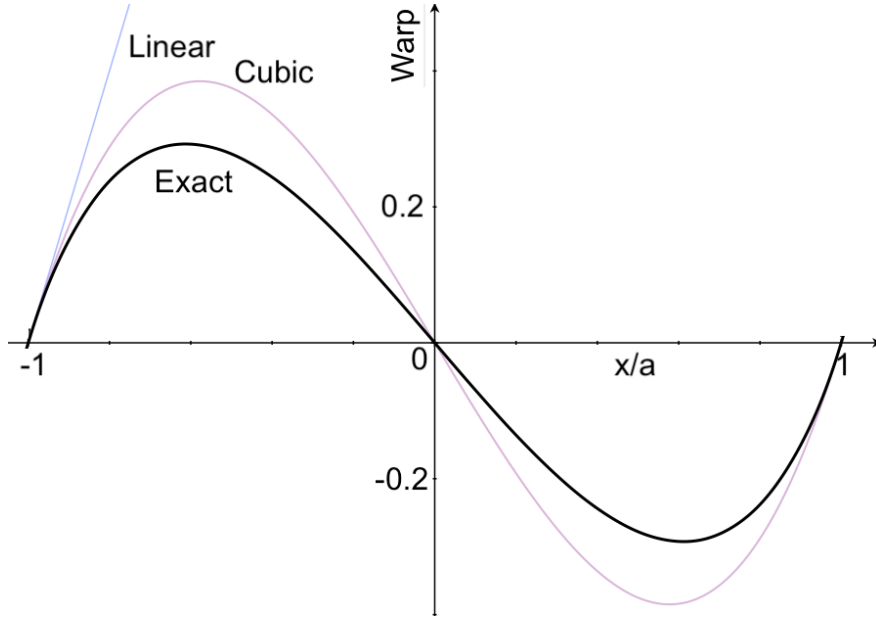


Figure 2: Normalized warp $\frac{u_z(x,y)}{\theta a^2}$ of a cross section of a classically elastic square bar vs. position on the surface. Comparison of exact solution, equation 2; linear corner solution, equation 3; and cubic corner solution equation 4.

If one admits fifth order terms, the warp becomes

$$u_z = \theta \frac{1}{16a^2} \left(C_1(x^3y - xy^3) + \frac{C_2}{a^2}(x^5y - xy^5) \right) \quad (7)$$

with $C_1 = 5$ and $C_2 = 33/38$ after [10]. Here the coordinates are not normalized. This result, obtained via an energy minimization procedure, predicts a torsional rigidity only 0.05% higher than the classical exact value [3]. The predicted warp near the corner is, however, about 15% lower than that of the exact solution. The energy method is comparatively insensitive to the corner because stress tends to zero there.

3 Cosserat elasticity

3.1 Corner element: qualitative

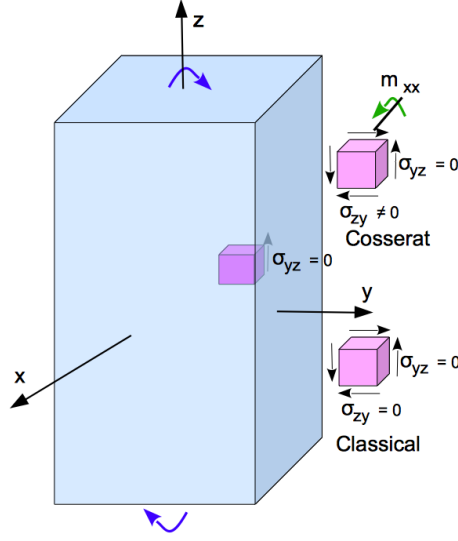


Figure 3: Stress can be asymmetric and nonzero at the corner of a cross section of a Cosserat elastic square cross section bar in torsion.

The corner element is instructive for Cosserat elasticity as well as classical elasticity. The corner element allows nonzero shear stress and strain because, as shown in Figure 3, asymmetry in the stress can be balanced by a distributed moment which occurs in Cosserat solids. The moment is driven by gradients in local rotation which in turn are coupled to the rotation associated with displacement gradients. Detailed analysis of the Cosserat case is, however, not so simple as in the classical case.

3.2 Governing equations

Cosserat elasticity has six isotropic elastic constants, $G, \lambda, \alpha, \beta, \gamma$ and κ . G is the shear modulus observed in the absence of strain gradients; λ is the Lamé elastic constant of classical elasticity. Constants α, β, γ govern sensitivity to rotation gradients; κ quantifies the coupling between the local or micro rotation field with ϕ with the rotation associated with displacement gradients. The constitutive equations for a linear isotropic Cosserat elastic solid [14] [15] are as follows.

$$\sigma_{ij} = 2G\epsilon_{ij} + \lambda\epsilon_{kk}\delta_{ij} + \kappa e_{ijk}(r_k - \phi_k) \quad (8)$$

$$m_{ij} = \alpha\phi_{k,k}\delta_{ij} + \beta\phi_{i,j} + \gamma\phi_{j,i} \quad (9)$$

In Cosserat elasticity the stress, σ_{ij} , can be asymmetric. The moment that results from asymmetry is balanced by a couple stress, m_{ij} . The antisymmetric part of the stress is related to local rotations: $\sigma_{jk}^{antisym} = \kappa e_{jkm}(r_m - \phi_m)$ in which ϕ_m is the rotation of points, called micro-rotation, e_{jkm} is the permutation symbol, and $r_k = \frac{1}{2}e_{klm}u_{m,l}$ is the macro-rotation based on the antisymmetric part of gradient of displacement u_i .

Technical constants obtained from the tensorial elastic constants are beneficial for physical insight. They are as follows.

$$\text{Young's modulus } E = \frac{2G(3\lambda + 2G)}{2\lambda + 2G} \quad (10)$$

$$\text{Shear modulus } G \quad (11)$$

$$\text{Poisson's ratio } \nu = \frac{\lambda}{2(\lambda + G)} \quad (12)$$

$$\text{Characteristic length, torsion } \ell = \sqrt{\frac{\beta + \gamma}{2G}} \quad (13)$$

$$\text{Characteristic length, bending } \ell_b = \sqrt{\frac{\gamma}{4G}} \quad (14)$$

$$\text{Coupling number } N = \sqrt{\frac{\kappa}{2G + \kappa}} \quad (15)$$

$$\text{Polar ratio } \Psi = \frac{\beta + \gamma}{\alpha + \beta + \gamma}. \quad (16)$$

Physically, the couple stress arises from twisting or bending of micro-structural elements within the material. For foams and rib lattices, the origin of such moments is readily visualized. The characteristic lengths ℓ_t and ℓ_b represent length scales at which couple stress is strongly manifested. If a specimen or a heterogeneity in a specimen is on the order of the characteristic lengths, less than a factor of 10 or 20 larger, deviations from classical elasticity are observed. The coupling number N quantifies the degree of coupling between macro and micro rotation fields. The polar ratio Ψ provides a ratio of rotation sensitivity in different directions analogous to Poisson's ratio in classical elasticity.

Equilibrium equations [15] for force and moment in the Cosserat solid are, respectively,

$$\sigma_{ij,i} = 0 \quad (17a)$$

$$m_{ij,i} + e_{jkl}\sigma_{kl} = 0. \quad (17b)$$

For many purposes it is expedient to use field equations obtained from the constitutive equations 8, 9 and the equilibrium equations 17.

The following three of the six field equations are satisfied [10] for the assumed torsional deformation equations 1.

$$(2G + \lambda)u_{x,xx} + (G + \frac{\kappa}{2})(u_{x,yy} + u_{x,zz}) + (G + \lambda - \frac{\kappa}{2})(u_{y,xy} + u_{z,xz}) + \kappa(\phi_{z,y} - \phi_{y,z}) = 0 \quad (18a)$$

$$(G - \frac{\kappa}{2} + \lambda)(u_{x,xy} + u_{z,yz}) + (G + \frac{\kappa}{2})(u_{y,xx} + u_{y,zz}) + (2G + \lambda)u_{y,yy} + \kappa(\phi_{x,z} - \phi_{z,x}) = 0 \quad (18b)$$

$$(G - \frac{\kappa}{2} + \lambda)(u_{x,xz} + u_{y,yz}) + (G + \frac{\kappa}{2})(u_{z,xx} + u_{z,yy}) + (2G + \lambda)u_{z,zz} + \kappa(\phi_{y,x} - \phi_{x,y}) = 0 \quad (18c)$$

For the torsional displacements, the remaining three field equations become

$$(G + \frac{\kappa}{2})(u_{z,xx} + u_{z,yy}) + \kappa(\phi_{y,x} - \phi_{x,y}) = 0 \quad (19)$$

$$(\alpha + \beta + \gamma)\phi_{x,xx} + (\alpha + \beta)\phi_{y,xy} + \gamma\phi_{x,yy} + \kappa(u_{z,y} - \theta x - 2\phi_x) = 0 \quad (20)$$

$$(\alpha + \beta + \gamma)\phi_{y,yy} + (\alpha + \beta)\phi_{x,xy} + \gamma\phi_{y,xx} - \kappa(u_{z,x} + \theta y + 2\phi_y) = 0. \quad (21)$$

3.3 Corner element analysis

Analysis of warp of a Cosserat solid at the corner is as follows.

If the warp is a linear function of x and y following the classical example, equation 3, the macro-rotation $r_x = (-C_1 a - x)$ is a linear function. If we have $\phi_x = r_x$, which is possible because the allowable limit $\kappa \rightarrow \infty$ requires the rotations to be equal, then the boundary condition on stress is satisfied. But via equation 9, the couple stress for the x direction is

$$m_{xx} = (\alpha + \beta + \gamma)\phi_{x,x} + \alpha(\phi_{y,y} + \phi_{z,z}). \quad (22)$$

A linear function for ϕ_x gives a constant m_{xx} but at the boundary, one must have $m_{xx} = 0$ because it is a free surface. To satisfy the boundary condition, the constant must be zero so there is no couple stress m_{xx} that could balance an asymmetric stress σ_{yz} . There is not enough freedom in an assumed micro-rotation ϕ_x linear in x . More freedom is provided via more terms in ϕ .

As was done in the classical case, assume the warp to have a sigmoid cubic form

$$u_z = \theta \frac{C_1}{2a^2} (x^3 y - x y^3), \quad (23)$$

in which C_1 is to be determined; it has a value of 1 in the classical case. The macro-rotations are

$$r_x = \frac{\theta}{2} \left(\frac{C_1}{2a^2} (x^3 - 3xy^2) - x \right), \quad r_y = \frac{\theta}{2} \left(-\frac{C_1}{2a^2} (3x^2 y - y^3) - y \right), \quad r_z = \theta z \quad (24)$$

The micro-rotation is assumed, following [10], to have the form

$$\frac{\phi_x(x, y)}{\theta} = f_1 x + f_2 x^3 + f_3 x y^2 + f_4 x^5 + f_5 x^3 y^2 + f_6 x y^4 \quad (25)$$

$$\frac{\phi_y(x, y)}{\theta} = f_1 y + f_2 y^3 + f_3 x^2 y + f_4 y^5 + f_5 x^2 y^3 + f_6 x^4 y \quad (26)$$

$$\frac{\phi_z(x, y)}{\theta} = z \quad (27)$$

The field equations 19, 20, 21 cannot be satisfied by individual polynomial terms. They may be satisfied exactly by an infinite series or approximately by a finite series of such terms. For Cosserat elasticity only approximate solutions [9] [10] are available for the square cross section bar. Because the focus here is upon the corner element, it is assumed that $x = a$ and $y = a$. At the corner, equations 20, 21 become equivalent.

However, if for simplicity only terms f_1, f_2, f_3 are retained then the boundary condition on couple stress m_{xy} ,

$$m_{xy} = [\beta \phi_{x,y} + \gamma \phi_{y,x}] |_a = 0 \quad (28)$$

cannot be satisfied because terms f_1 and f_2 do not contribute so f_3 is forced to zero because ϕ_x cannot be zero unless $\kappa = 0$. Therefore more terms are needed. Including f_4 has no effect on equation 28. Including f_5 allows one to satisfy equation 28 provided the f_5 and f_3 terms cancel in equation 25.

There must also be sufficient freedom to satisfy the boundary condition on m_{xx} ,

$$m_{xx} = [(\alpha + \beta + \gamma)\phi_{x,x} + \alpha(\phi_{y,y} + \phi_{z,z})] |_a = 0 \quad (29)$$

so f_6 is included.

If $\kappa \rightarrow \infty$ ($N \rightarrow 1$) then $\phi \rightarrow r$. If the warp is of the form in equation 23, then the micro-rotation ϕ can have the same functional dependence as the macro-rotation r from the displacement

gradient only if f_1, f_2, f_3 are nonzero. To obtain the same functional dependence, make the following assumption, for all N . There is sufficient freedom remaining to do this.

$$f_1 = \frac{2}{3}a^2 f_3, \quad f_2 = -\frac{1}{3}f_3 \quad (30)$$

The boundary condition on m_{xy} , Equation 28, implies

$$f_6 = -\frac{1}{2}f_5 - \frac{1}{2}\frac{1}{a^2}f_3 \quad (31)$$

The boundary condition on m_{xx} , Equation 29, gives, at the corner,

$$[(2\alpha + \beta + \gamma)(f_1 + 3f_2a^2 + f_3a^2 + 5f_4a^4 + 3f_5a^4 + f_5a^4) + \alpha] |_{a=0} = 0 \quad (32)$$

This is considerably simplified if one assumes $\alpha = 0$, equivalently, $\Psi = 1$. In prior analyses, Ψ has little effect, and none at all if $N = 1$ as is the case for some materials studied in experiments. The field equation 19 is satisfied at the corner.

Let $f_4 = 0$ because it is not needed. The field equation 20 then gives

$$\theta[(\alpha + \beta + \gamma)(6f_2a + 6f_5a^3) + (\alpha + \beta)(2f_3a + 6f_5a^3 + 4f_6a^3) + \gamma(2f_3a + 2f_5a^3 + 12f_6a^3)] = -\kappa(r_x - \phi_x) \quad (33)$$

At the corner, field equation 21 is equivalent to equation 20.

Incorporating the definitions of the characteristic lengths, equations 13 and 14, the interrelation equations 31 30 and with the assumption $\Psi = 1$,

$$f_3 \left(-l_t^2 \frac{16}{15} - 8l_b^2 \right) = -\kappa(r_x - \phi_x). \quad (34)$$

The boundary condition on shear stress $\sigma_{yz}|_{a=0} = 0$ gives

$$G\theta a(1 - C_1) = -\kappa(r_x - \phi_x). \quad (35)$$

The simplified field equation 21 is combined with the boundary condition, equation 35 on shear stress. Incorporate $r_x|_{a=0} = (C_1 - 1)a\theta$. Setting the boundary condition equation equal to the field equation gives C_1 . Summing these equations gives f_3 . From the result, C_1 in warp equation 23 is found to be, for $\Psi = 1$,

$$C_1 = 1 - f_3 \left(-l_t^2 \frac{16}{15} - 8l_b^2 \right). \quad (36)$$

in which

$$f_3 = \frac{-2}{\frac{1}{2} \left(\frac{1+N^2}{N^2} \right) \left(\frac{16}{15}l_t^2 + 8l_b^2 \right) + \frac{23}{30}a^2}. \quad (37)$$

The present corner solution, similarly to the approximate solutions of [9], [10], predicts warp to be reduced is a Cosserat solid compared with a classical solid. The warp is reduced progressively more as l_t becomes larger and as N becomes larger. The curves in Figure 4 from the present solution are shown in the vicinity of the corner for $l_t/a = 0, 0.1, 0.2$ and for $l_b = 0.5l_t, l_b = 0.707l_t$. It is assumed that $N = 1$ and that $\Psi = 1$. An increase in l_b further reduces the warp in the vicinity of the corner. In plots of warp for various elastic constants, the range chosen is within the limits for

stability. In classical elasticity the shear modulus and bulk modulus must be positive. In Cosserat solids, the range for stability corresponds to $\ell_b > 0$; $\kappa > 0$ implies $N > 0$; with the definition of N and considering the limit of large κ , $0 < N < 1$. Because $-\gamma < \beta < \gamma$, the characteristic length in bending follows $\ell_b > \frac{1}{2}\ell_t$.

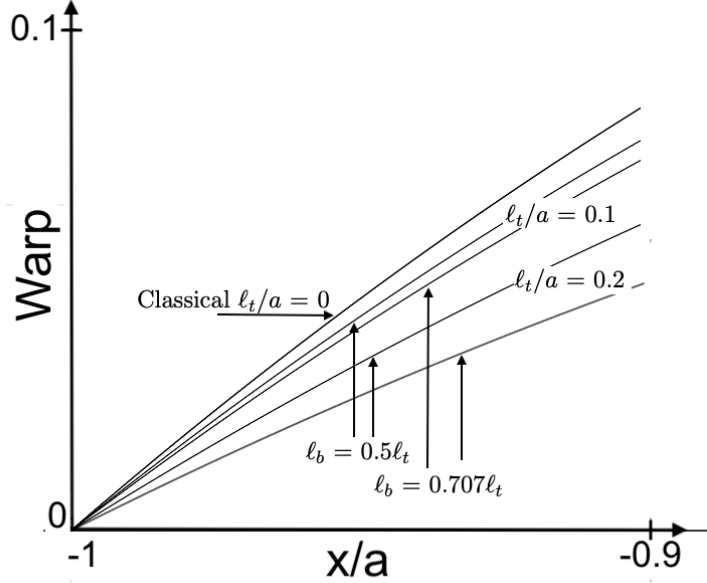


Figure 4: Normalized warp $\frac{u_z(x,y)}{\theta a^2}$ near a corner of a cross section of a square bar, classical ($\ell_t/a = 0$) and Cosserat.

Warp from present corner analysis, $\ell_t/a = 0, 0.1, 0.2$; $\ell_b = 0.5\ell_t$, $\ell_b = 0.707\ell_t$; $N = 1$; $\Psi = 1$.

In view of the complexities encountered even at the corner, it is natural to consider making simplifying assumptions at the outset. For example, $r_j = \phi_j$ corresponds to the couple stress [16] theory, and the limit $N = 1$ in Cosserat elasticity. From equation 24 for r_j , the terms in equation 25 for ϕ_x must include only f_1, f_2, f_3 but then the boundary condition equation 28 cannot be satisfied because terms f_1 and f_2 do not contribute so f_3 is forced to zero. Consequently $\phi_x = 0$ and it cannot equal r_x as assumed. Therefore the warp, hence r_x , must have more terms than originally assumed. So the shape of the assumed warp curve does not suffice to satisfy the boundary condition even if one can adjust the magnitude and slope via C_1 . The Cosserat solid is unlike the classical solid in this respect.

4 Discussion

Warp in the torsion of square cross section is reduced in a Cosserat solid in comparison with a classical solid. This implies that the concentration of stress is reduced in a Cosserat solid, potentially giving rise to a greater toughness.

Cosserat effects become substantial when the size scale of the specimen is not too much greater than the characteristic length. There is a length scale associated with the corner as well; in a real material, the corner cannot be perfectly sharp. There is the limitation associated with the spacing between atoms, and possibly associated with larger heterogeneity in the material.

Warp is also of interest as an experimental modality for the study of Cosserat solids. Cosserat elastic constants have been obtained experimentally in bone [17], foams [13, 18] and lattices [19] using the predicted size effects in the torsional [20] and bending [21] rigidity of round rods. The method is painstaking in that it requires repeated measurements on specimens of progressively smaller diameter. The Cosserat characteristic length was also found experimentally in a two-dimensional polymer honeycomb [22]. Study of corner deformation [23] or strain distributions [24] or warp [25] in the torsion of a square bar allows inferences to be made from measurements on a single specimen.

Generalized continuum properties of heterogeneous materials may be obtained by homogenization analysis as well as experiment. Cosserat elastic constants have been obtained for rib lattices [26, 27] and for composites [28]; homogenization was also done in the context of second gradient generalized continuum theory [29].

Exact analytical solutions for interpretation of experiments are available for circular cylinders of Cosserat solids, but for square cross section bars, only approximate solutions are available. The approximate solutions are complicated for the full set of Cosserat constants. To compare their accuracy, observe that the Cosserat solution must reduce to the classical solution for $\ell_t = 0$ or for $N = 0$. The warp predicted by energy minimization [10] at the center is 5% greater than the classical value but near the corner it is about 15% lower than that of the exact classical value. The present corner solution reduces to the exact classical warp for $\ell_t = 0$ or for $N = 0$. The approximate solution [9] also reduces to classical elasticity for $\ell_t = 0$ or for $N = 0$. These are likely to be more accurate for small values of ℓ_t ; the energy minimization approach is superior for large ℓ_t .

The slope of the warp from the corner solution is similar to the slope for the full approximate solution for small ℓ_t/a . For larger ℓ_t/a , the corner solution predicts a greater reduction in warp than does the full solution. In the corner solution, the warp actually reverses if $\ell_t/a = 0.5$ but remains positive in the full solution. Therefore the corner solution is limited in its range of applicability.

Higher order terms are needed for the Cosserat solid to satisfy field and boundary conditions even if it is only at the corner. Recall that the field equations cannot be satisfied over the cross section by individual polynomial terms. Higher order terms entail nonlocal response, hence sensitivity to deformation far from the corner. That is why the solution for the corner is reasonable only if ℓ_t is not too large. As for uniqueness of solution, the proofs of uniqueness apply to exact solutions, not approximate solutions. Therefore it is not surprising that there is choice of how to satisfy the conditions at the corner.

5 Conclusions

The corner of a square bar in torsion has zero stress and strain in a classical solid but nonzero stress and strain in a Cosserat solid. This is easy to demonstrate in classical elasticity; moreover the slope of the warp curve near the corner is obtained quantitatively using a simple cubic approximation to the warp. In Cosserat elasticity an approximate solution is obtained for the slope the warp curve at the corner. Warp is reduced in a Cosserat solid compared with a classical solid. The solution reduces properly to classical elasticity for zero characteristic length ℓ_t but predicts too much warp reduction for large ℓ_t . The energy based solution is superior for that case.

The author gratefully acknowledges support of this research by the U.S. National Science Foundation via Grant No. CMMI -1906890

References

- [1] E. Reissner, Note on the theorem of the symmetry of the stress tensor. *J. Math. Phys.* **23**, 192-194 (1944).
- [2] D. B. Bogy and E. Sternberg, The effect of couple stresses on the corner singularity due to an asymmetric shear loading, *Int. J. Solids Structures* **4**, 159-174, (1968).
- [3] S. Timoshenko and J. N. Goodier, *Theory of Elasticity*, McGraw-Hill, New York (1970).
- [4] N. J. Freeman, and L. M. Keer, Torsion of a Cylindrical Rod Welded to an Elastic Half Space, *J. Appl. Mech.*, **34**(3): 687-692 (6 pages) 1967
- [5] R. A. Westmann, Torsion of a Cylindrical Rod Welded to an Elastic Half Space, comment, *J. Appl. Mech.*, **35**, 197, (1968).
- [6] L. M. Keer and N. J. Freeman, Load transfer problem for an embedded shaft in torsion *J. Appl. Mech.* , **37**(4): 959-964 (1970).
- [7] S. Shahzad and F. Dal Corso, Torsion of elastic solids with sparse voids parallel to the twist axis. *Mathematics and Mechanics of Solids* **24**(7), 2126-2153. (2019)
- [8] I. S. Sokolnikoff, *Theory of Elasticity*, Krieger, Malabar, FL, (1983).
- [9] H. C. Park and R. S. Lakes, Torsion of a micropolar elastic prism of square cross section. *Int. J. Solids, Structures*, **23**, 485-503 (1987).
- [10] W. J. Drugan and R. S. Lakes, Torsion of a Cosserat elastic bar of square cross section: theory and experiment, *Z. Angew. Math. Phys.*, **69**(24), 24 pages (2018).
- [11] R. D. Mindlin, Effect of couple stresses on stress concentrations, *Experimental Mechanics*, **3**, 1-7, (1963).
- [12] L. J. Gibson and M. F. Ashby, *Cellular Solids*, Pergamon, Oxford, 1988; 2nd Ed., Cambridge University press, Cambridge, (1997).
- [13] Z. Rueger and R. S. Lakes, Experimental Cosserat elasticity in open-cell polymer foam, *Philosophical Magazine*, **96**(2), 93-111 (2016).
- [14] E. Cosserat, and F. Cosserat, *Theorie des Corps Deformables*, Hermann et Fils, Paris (1909).
- [15] A. C. Eringen, Theory of micropolar elasticity. In *Fracture Vol. 1*, 621-729 (edited by H. Liebowitz), Academic Press, New York (1968).
- [16] W. T. Koiter, Couple-Stresses in the theory of elasticity, Parts I and II, *Proc. Koninklijke Ned. Akad. Wetenschappen* **67**, 17-44 (1964).
- [17] J. F. C. Yang and R. S. Lakes, Experimental study of micropolar and couple stress elasticity in bone in bending, *Journal of Biomechanics*, **15**, 91-98, (1982).
- [18] Z. Rueger and R. S. Lakes, Cosserat elasticity of negative Poisson's ratio foam: experiment, *Smart Materials and Structures* **25**(5) (2016).
- [19] Z. Rueger and R. S. Lakes, Strong Cosserat elasticity in a transversely isotropic polymer lattice, *Phs. Rev. Lett.*, **120**, 065501, (2018).
- [20] R. D. Gauthier and W. E. Jahsmann, A quest for micropolar elastic constants. *J. Appl. Mech.*, **42**, 369-374 (1975).
- [21] G. V. Krishna Reddy, and N. K. Venkatasubramanian, On the flexural rigidity of a micropolar elastic circular cylinder, *J. Applied Mechanics* **45**, 429-431 (1978).
- [22] R. Mora and A. M. Waas, Measurement of the Cosserat constant of circular cell polycarbonate honeycomb, *Philos. Mag. A*, **80** 1699 - 1713 (2000).
- [23] R. S. Lakes, D. Gorman, and W. Bonfield, Holographic screening method for microelastic solids, *J. Materials Science*, **20**, 2882-2888, (1985).
- [24] H. C. Park and R. S. Lakes, Cosserat micromechanics of human bone: strain redistribution by a hydration-sensitive constituent, *J. Biomechanics*, **19** 385-397 (1986).

- [25] W. B. Anderson, R. S. Lakes, and M. C. Smith, Holographic evaluation of warp in the torsion of a bar of cellular solid, *Cellular Polymers*, 14, 1-13, (1995).
- [26] T. Tauchert, A Lattice Theory for Representation of Thermoelastic Composite Materials, *Recent Adv. Eng. Sci.*, 5(1), 325-345, (1970)
- [27] Z. P. Bazant and M. Christensen, Analogy between micropolar continuum and grid frameworks under initial stress. *Int. J. Solids Struct.* 8, 327-346 (1972).
- [28] D. Bigoni and W. J. Drugan, Analytical derivation of Cosserat moduli via homogenization of heterogeneous elastic materials, *J. Appl. Mech.*, 74, 741-753 (2007).
- [29] A. Bacigalupo, M. Paggi, F. Dal Corso, and D. Bigoni, Identification of higher-order continua equivalent to a Cauchy elastic composite, *Mechanics Research Communications*, 93, 11-2, (2018).